

# Diffusion and Phase Transformations During Interfacial Reaction Between Lead-Tin Solders and Palladium

G. GHOSH

Department of Materials Science and Engineering, Robert R. McCormick School of Engineering and Applied Science, Northwestern University, 2225 N. Campus Dr., Evanston, IL 60208-3108

The interfacial reaction between Pb-Sn solders and bulk Pd substrate is studied both in the liquid- and solid-state of the solder. The interfacial microstructures are characterized by imaging and energy dispersive x-ray analysis in scanning electron microscope. The correlation between the diffusion path and interfacial microstructure in 62Sn38Pb/Pd, 95Pb5Sn/Pd, and Pb/Pd diffusion couples is demonstrated by means of calculated isothermal sections of the Pb-Sn-Pd system and the metastable phase diagram of the Pb-Pd system.

**Key words:** Diffusion path, interdiffusion, interfacial reaction, intermetallic, palladium, solder

## INTRODUCTION

The strength and interfacial properties of the solder joints are determined by the interfacial microstructure. The evolution of interfacial microstructure in solder joints is governed by the diffusion path during processing and in service. Recently, the microelectronics industry has shown significant interest in palladium surface finish in interconnects.<sup>1</sup> Therefore, it is desirable to understand the interfacial reaction between solders and palladium. In order to predict the diffusion path and microstructural evolution, it is necessary to have a good thermodynamic description and the kinetic parameters of the phases in the system of interest. While there are many binary, ternary, and multicomponent solders of practical interest, the ternary and multicomponent phase diagrams are needed to understand the interfacial reaction between solder and substrate. In a majority of the cases such phase diagrams are not known. The thermodynamic description of one of the ternary systems of interest, Pb-Sn-Pd, has recently been reported.<sup>2</sup>

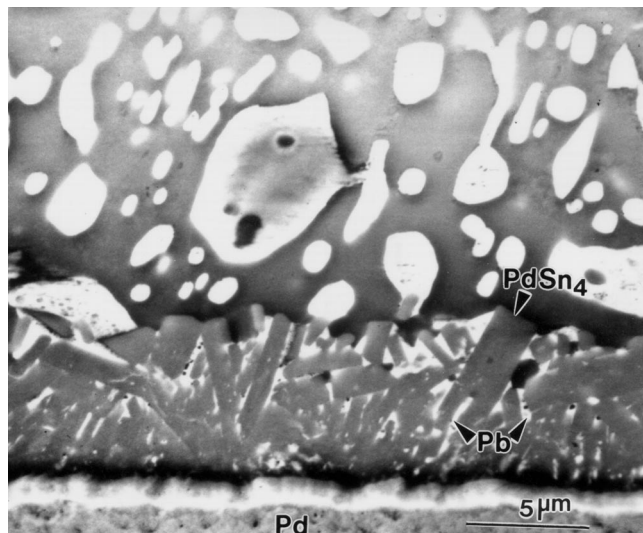
Even though Pd is present as a thin layer in electronic packaging component such as lead frame, thick films of alloys containing Pd are used in ceramic packages. A systematic study of bulk diffusion couples should be considered as a first step toward understanding the diffusion path and the interfacial reac-

tion between Pb-Sn solders and Pd or Pd-containing alloys. A diffusion path is defined by the average composition in a direction perpendicular to the original interface of the diffusion couple. For a given ternary isothermal section, Kirkaldy and Brown<sup>3</sup> have developed a set of rules for the construction of diffusion paths. At a constant temperature and pressure, Kirkaldy and Brown<sup>3</sup> predicted that a ternary diffusion couple will exhibit only one diffusion path which will be dictated by the thermodynamic and kinetic parameters. However, since the kinetic data is not available for the Pb-Sn-Pd system, it is necessary to determine diffusion paths experimentally. Therefore, the objectives of this research are to carry out a systematic study of interfacial reaction using diffusion couples of Pb-Sn solders and bulk Pd and to correlate the interfacial microstructure with the calculated phase diagrams.

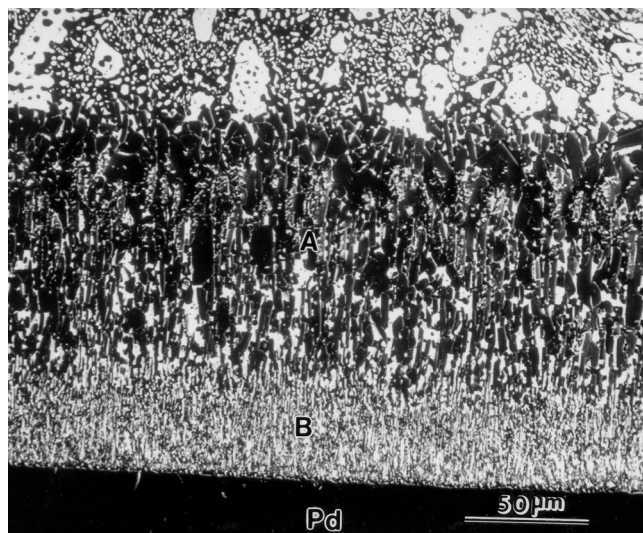
## EXPERIMENTAL PROCEDURE

Raw materials of following purity were obtained from Alfa-Aesar: Pb (99.999 wt.%), Pd (99.95 wt.%), and Sn (99.999 wt.%). A eutectic solder (62Sn38Pb), a high-Pb solder (95Pb5Sn) were prepared by melting the pure elements in evacuated and sealed quartz tubes. Polished (to 1  $\mu\text{m}$ ) palladium foils (0.5 mm thick, 17  $\times$  17 mm<sup>2</sup>) were used as substrates. The eutectic solder, the high-Pb solder, and pure Pb were used for interfacial reaction studies. Sessile drop experiments were carried out in air using RMA flux

(Received February 18, 1998; accepted August 10, 1998)



a

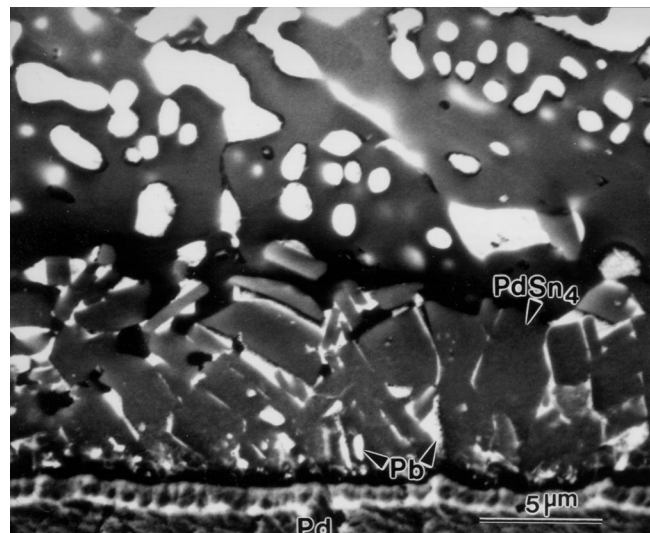


b

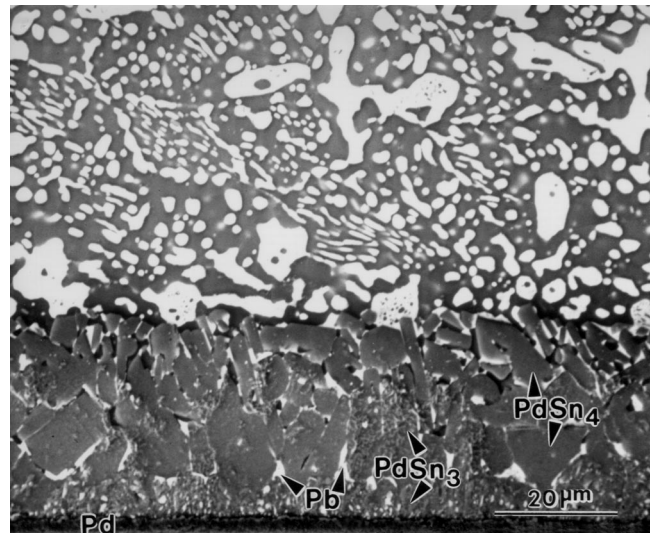
Fig. 1. Backscattered SEM micrographs showing composite interfacial microstructures after liquid-state reaction between 62Sn38Pb solder and Pd: (a) at 220°C for 50s, and (b) at 220°C for 30 min. The latter shows two distinct regions (marked A and B).

(Kester-186). For the eutectic solder, liquid-state reaction was carried out either at 220°C for 50 s or at 260°C for 5 s. These temperature-time combinations were chosen to mimic a typical reflow and wave soldering process, respectively. Additional longer time reactions were also performed. For the high-Pb solder, the liquid-state reaction was carried out at 325°C for 10 and 60 s. For pure Pb, the liquid-state reaction was carried out at 343°C for 15 and 35 s. Since the microstructure of the solder joints is also affected by diffusion in the solid-state (in service), selected diffusion couples were subjected to solid-state reaction at 125°C for up to 60 days.

Microstructural characterization was carried out in a HITACHI S-4500 scanning electron microscope (SEM) with cold field-emission gun and a Noran energy dispersive x-ray (EDS) detector and necessary



a



b

Fig. 2. Backscattered SEM micrographs showing interfacial microstructures of 62Sn38Pb solder on Pd: (a) at 260°C for 5 s, and (b) at 220°C for 60 s.

software/database for composition analysis or in a HITACHI S-540 SEM with a backscattered detector. Both SEMs were operated at 20 kV. In S-4500 SEM, the micrographs were acquired digitally using the lower detector, whereas polaroid films were used in the S-540 SEM. Composition profiles across the diffusion zones were obtained either in the area mode (macroscopic) or in the point mode (microscopic).

## RESULTS

Figure 1 shows the interfacial microstructures after liquid-state reaction, eutectic solder (62Sn38Pb) on Pd, at 220°C for 50 s (1a) and at 220°C for 30 min (1b). Figure 1a shows a composite microstructure in the interdiffusion zone, about 6 µm in thickness, consisting of highly faceted intermetallic and (Pb) phases. By EDS analysis, the intermetallic phase was confirmed to be PdSn<sub>4</sub>. It may be noted that the (Pb)

phase prefers to co-exist along the faceted surfaces of  $\text{PdSn}_4$ . This could be due to a specific orientation relationship and/or anisotropic interfacial energy between the Pb and  $\text{PdSn}_4$ . Figure 1b shows the interdiffusion zone after 30 min of reaction at  $220^\circ\text{C}$ . The total width of the interdiffusion zone is about  $140\ \mu\text{m}$ , and it consists of two distinct regions (marked A and B). The region A consists of  $\text{PdSn}_4$  and (Pb) and the region B consists of  $\text{PdSn}_3$  and (Pb). Figure 1b shows that a vast majority of the intermetallic grains exhibit columnar growth. Also, the  $\text{PdSn}_3$  grains are much finer than the  $\text{PdSn}_4$  grains. As seen in Fig. 1b, and also confirmed by EDS analysis, the fraction of (Pb) phase in the region B is much higher than that in the region A. Furthermore, the region A is almost twice as thick as the region B.

Figure 2a shows the interfacial microstructure after reaction at  $260^\circ\text{C}$  for 5 s, which is qualitatively similar to the microstructure shown in Fig. 1a. The faceted crystals shown in Fig. 2a were predominantly  $\text{PdSn}_4$ , and a few  $\text{PdSn}_3$  crystals were also detected by SEM. Figure 2b shows the microstructure after reaction at  $260^\circ\text{C}$  for 60 s. The interfacial microstructure consists of relatively large and highly faceted  $\text{PdSn}_3$  and (Pb) phases.

Figure 3 shows the interdiffusion zone developed when the diffusion couple, eutectic solder/Pd, was subjected to a long time (30 days) solid-state reaction at  $125^\circ\text{C}$  after a short time reaction in the liquid-state (at  $220^\circ\text{C}$  for 50 s). The interdiffusion zone can be divided into three regions: the region A (adjacent to the solder) primarily consists of the (Pb) phase; the region B consists of  $\text{PdSn}_4$  and (Pb) phases; and the region C (adjacent to Pd substrate) consists of  $\text{PdSn}_3$

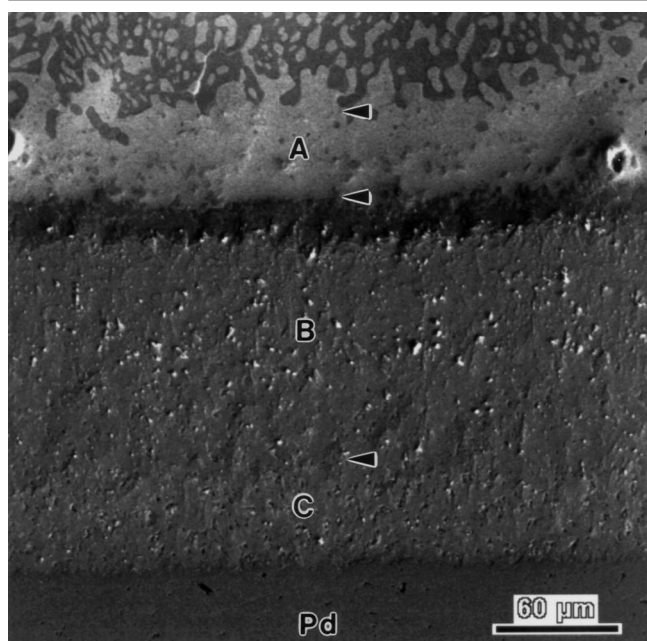


Fig. 3. SEM micrograph (with lower detector) showing interfacial microstructure, of 62Sn38Pb solder on Pd, developed after a long time (30 days) solid-state reaction at  $125^\circ\text{C}$ . The diffusion couple was made at  $220^\circ\text{C}$  for 50 s. The interdiffusion zone consists of three regions (marked A, B, and C).

and (Pb) phases. It is worth pointing out that the microstructures corresponding to the last two regions were also observed in Fig. 1b, i.e., after liquid state reaction at  $220^\circ\text{C}$  for 30 min.

The interfacial reaction between high-lead solder and Pd turned out to be complicated. Figure 4 shows a large interdiffusion zone after liquid-state reaction between the 95Pb5Sn solder and Pd at  $325^\circ\text{C}$  for 10 s. The width of the reaction zone was found to increase with reaction time. Except very close to the Pd-substrate where intermetallic could be observed (at a much higher magnification than shown in Fig. 4), the microstructure of the interdiffusion zone is suggestive of a decomposition reaction. Figure 5 is the composition profile across the reaction zone in Fig. 4. It clearly demonstrates extensive interdiffusion of Pb, Sn, and Pd over a considerable distance even after a short reaction time of 10 s. In order to investigate the origin of such decomposed microstructure, binary diffusion couple experiments with liquid Pb and Pd were performed. Since Pb melts at  $327^\circ\text{C}$ , the tem-

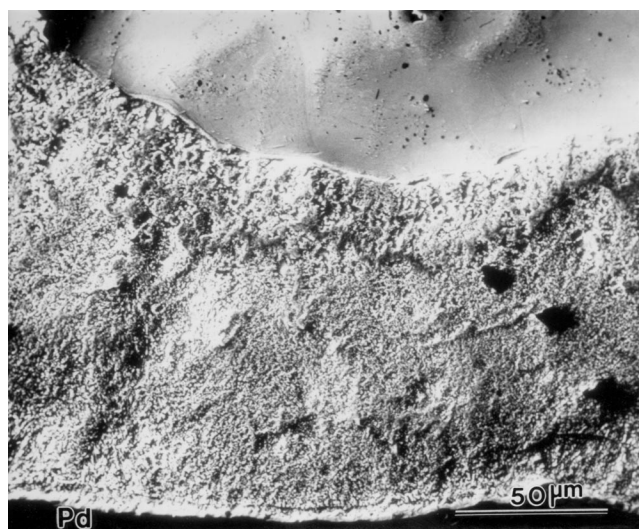


Fig. 4. SEM micrographs showing interfacial microstructures of 95Pb5Sn solder on Pd  $325^\circ\text{C}$  for 10 s.

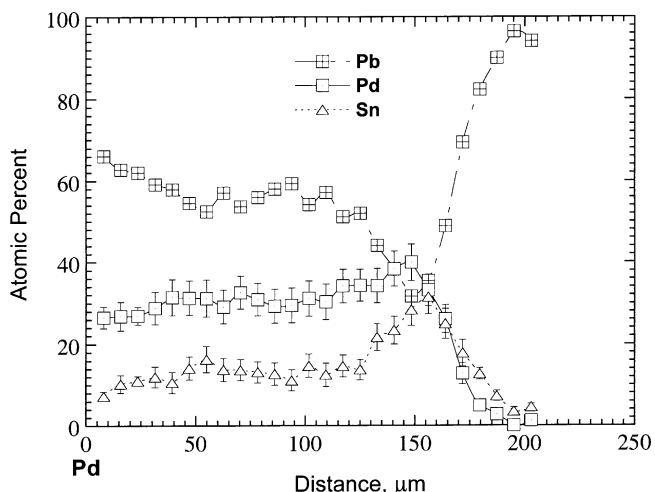
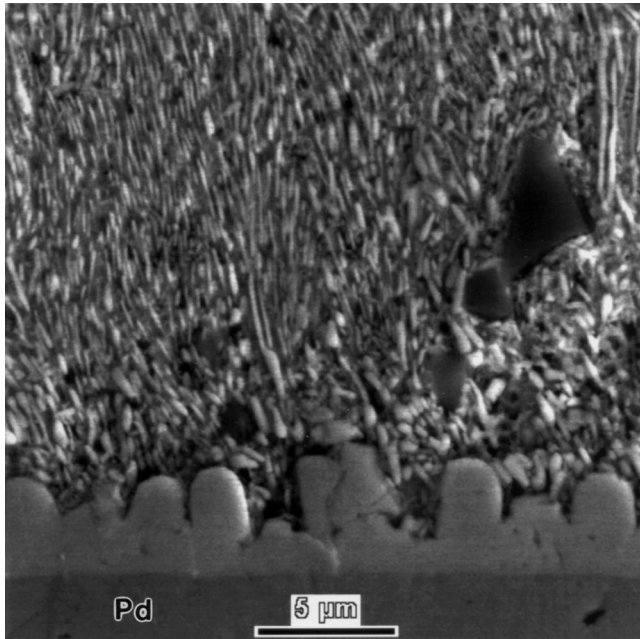
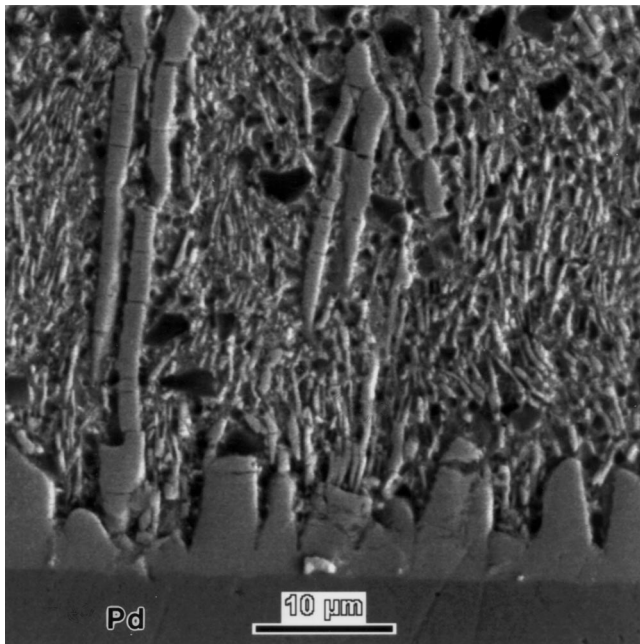


Fig. 5. Composite profile across the reaction zone in Fig. 4 showing extensive interdiffusion of Pb, Pd, and Sn.



a



b

Fig. 6. SEM micrograph showing bulk and interfacial microstructures after the reaction between liquid Pb and Pd (a) at 343°C for 15 s, and (b) at 343°C for 35 s.

perature of the binary diffusion couple experiment was slightly higher than that of the ternary diffusion couple 95Pb5Sn solder/Pd. Figures 6a and 6b show both interfacial and bulk microstructures after interfacial reaction between liquid-Pb and Pd. While a thin layer of PdPb<sub>2</sub> intermetallic layer may be seen adjacent to the Pd-substrate, the bulk microstructure of the reaction zone mainly consists of lamellar mixture of phases suggestive of eutectic solidification. A composition profile across the interdiffusion zone in the Pb/Pd couple in Fig. 7 demonstrates the evidence of

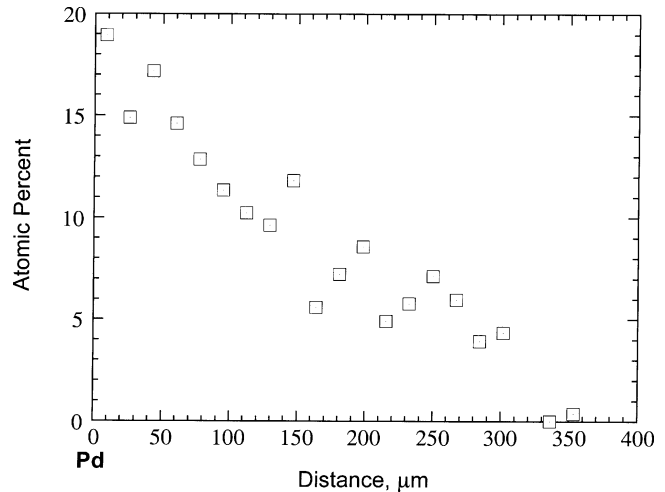


Fig. 7. Composition profile after reaction between liquid Pb and Pd at 343°C for 15 s. The profile provides the evidence for dissolution of Pd in liquid Pb.

Pd diffusion in the liquid Pb. Even though there is some uncertainty (due to the beam broadening in SEM) associated with the EDS analysis of such a fine scale microstructure, the chemical analysis showed that both phases were lead-rich; one containing less than 5 at.% Pd and the other containing about 25 at.% Pd. The latter value differs significantly from the Pd-content in the PdPb<sub>2</sub> phase.

The solid-state reaction of Pb/Pd and 95Pb5Sn/Pd diffusion couples also produced very different results. In the Pb/Pd diffusion couple, only PdPb<sub>2</sub> intermetallic was observed at the interface. This is expected from the Pb-Pd phase diagram if the interfacial reaction is controlled by the diffusion of Pd in Pb. However, the microstructural evolution of the 95Pb5Sn/Pd diffusion couple at 125°C was very different. Figure 8a is the backscattered SEM micrograph showing the microstructure of the interdiffusion zone of the 95Pb5Sn/Pd diffusion couple. A comparison of Fig. 8a with Fig. 4 suggests a significant microstructural change that has occurred at 125°C. In Fig. 8a, there is a region adjacent to the Pd-substrate suggestive of layered growth (marked X). However, a higher magnification of this layer, in Fig. 8b, showed a very fine scale phase mixture. The microstructure represents two different length scales; the larger length scale is due to phases present in the as-solidified state, and the smaller length scale represents the phases that have formed in the solid-state at 125°C.

## DISCUSSIONS

In a stable binary solution, each component always diffuses down its own chemical potential gradient, and the direction of the chemical potential gradient is always the same as that of the concentration gradient. However, the diffusion in a ternary system is much more complicated. In ternary and higher order systems, a higher chemical potential does not necessarily mean a higher concentration. It has been shown theoretically<sup>4</sup> and experimentally<sup>5</sup> that in metallic solid solutions that a component can inter-diffuse up

its own chemical potential gradient. This is possible even in an ideal solution due to correlation effects.<sup>6</sup> However, such an effect is not observed in metal-ceramic systems.<sup>7</sup>

In a binary diffusion couple, the product phase(s) after interfacial reaction can usually be predicted from the corresponding phase diagram. However, in ternary and multicomponent systems, it is not possible to predict the interfacial microstructure, or the phase sequence, or when the system will approach equilibrium unless the kinetic parameters are known. The complexity in ternary and higher-order systems is due to the additional degree(s) of freedom. While this may pose difficulty in the quantitative analysis of

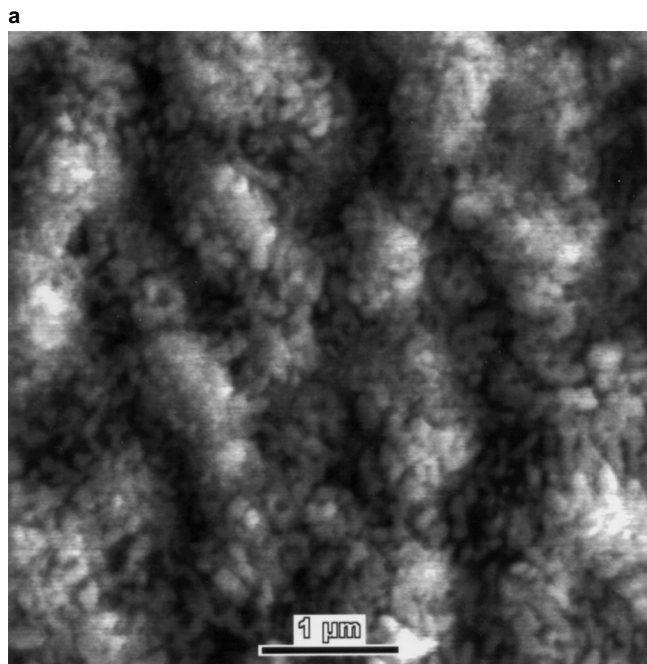
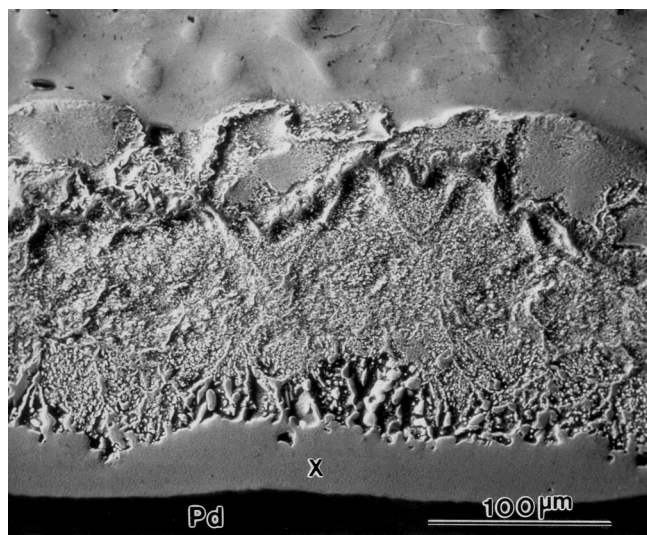


Fig. 8. SEM micrographs showing interfacial reaction after solid-state reaction: (a) 95Pb5Sn/Pd at 325°C for 10 s followed by 30 days at 125°C; and (b) a higher magnification image of the area marked X in (a).

transport kinetics in multicomponent systems, it may also be considered fortuitous for providing more degrees of freedom in material synthesis and controlling processing parameters. Nonetheless, a set of well-established principles<sup>7</sup> is available to interpret the interfacial microstructure governed by the diffusion path. These are: (a) Thermodynamic principle: If it is assumed that local equilibrium prevails, even after short reaction times, the neighboring phases in the interfacial microstructure must be given by the tie lines in the isothermal section. (b) Mass-balance principle: For a ternary diffusion couple in a closed system, the diffusion path in an isothermal section must intersect the initial composition vector (i.e., the straight line joining the initial end compositions) at least once. Violation of this rule implies that either there is a loss of material or misinterpretation of the results. (c) Kinetic principle: As a first approximation, one may assume that no component can diffuse up its own chemical potential gradient. Using these principles, one may rule out the unlikely diffusion paths, and the observed interfacial microstructure may be correlated with the calculated isothermal section.

Figure 9 shows the calculated isothermal section of the Pb-Sn-Pd system at 220°C. The solubility of Pd in liquid eutectic solder is less than 1 at.%. The presence of PdSn<sub>4</sub>+liquid, PdSn<sub>4</sub>+liquid+(Pb), PdSn<sub>4</sub>+(Pb), PdSn<sub>4</sub>+PdSn<sub>3</sub>+(Pb), and PdSn<sub>3</sub>+(Pb) phase fields may be noticed in Fig. 9. As Pd dissolves in the liquid solder, locally it becomes saturated and eventually PdSn<sub>4</sub> phase nucleates and grows near the interface. This is due to existence of the two-phase field PdSn<sub>4</sub>+liquid. As more Pd diffuses with time, the overall composition near the interface changes and enters the three-phase field PdSn<sub>4</sub>+liquid+(Pb). This is consistent with the microstructure in Fig. 1a where the existence of PdSn<sub>4</sub>+(Pb) in contact with solder (which was liquid at 220°C) may be noted. The observation of

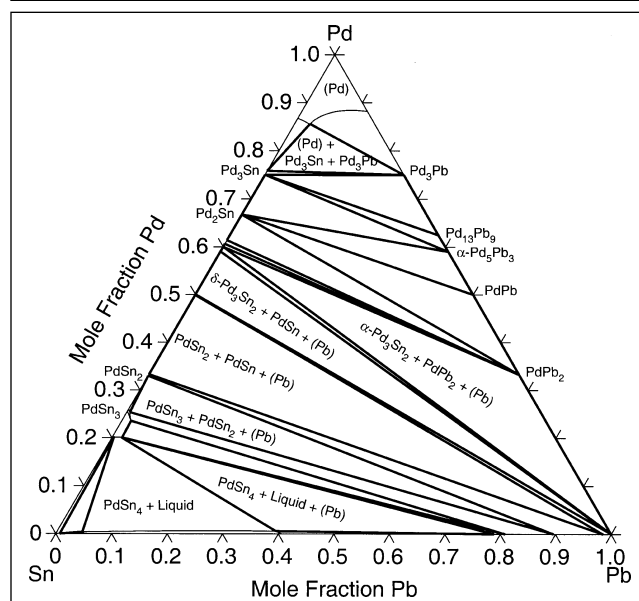


Fig. 9. Calculated isothermal section of the Pb-Sn-Pd system at 220°C.

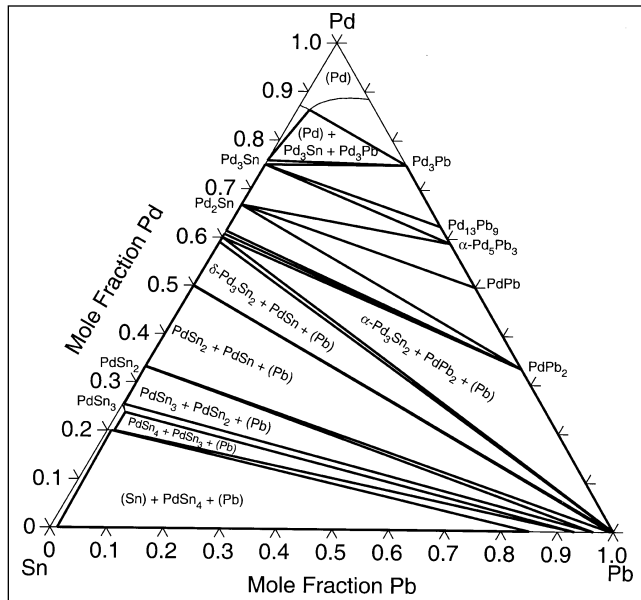


Fig. 10. Calculated isothermal section of the Pb-Sn-Pd system at 125°C.

Calculated Metastable Pb-Pd Phase Diagram

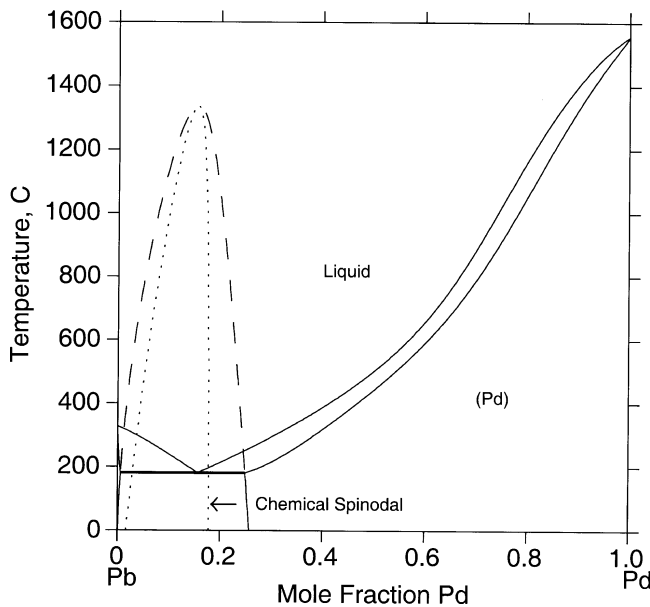


Fig. 11. Calculated metastable Pb-Pd phase diagram.

$\text{PdSn}_3 + (\text{Pb})$  phase mixture after prolonged reaction at 220°C (shown in Fig. 1b) is also consistent with the corresponding phase field shown in the calculated phase diagram in Fig. 9. These results suggest that the diffusion path follows along liquid/liquid+ $\text{PdSn}_4$ /liquid+ $\text{PdSn}_4 + (\text{Pb})$ / $\text{PdSn}_4 + (\text{Pb})$ / $\text{PdSn}_3 + \text{PdSn}_4 + (\text{Pb})$  phase fields in Fig. 9. This diffusion path is also consistent with the principles of local equilibrium and mass-balance mentioned above. Figure 10 shows the calculated isothermal section at 125°C. In the solid-state, the topology of the calculated isothermal section remains essentially the same. In other words, Fig. 10 can also be used at other temperatures pro-

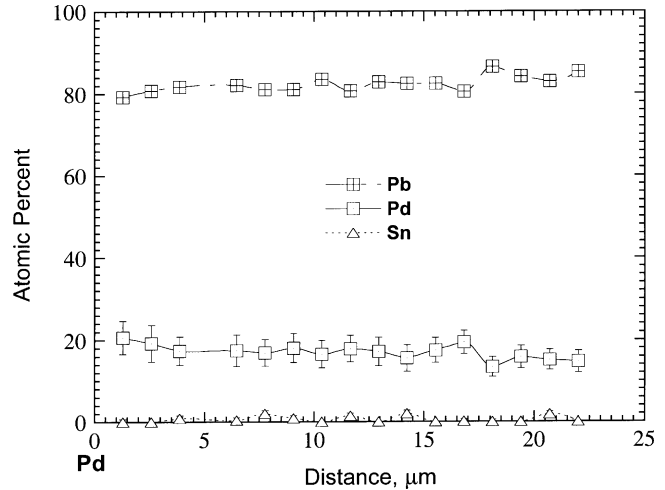


Fig. 12. Composition profile across the interfacial layer (marked X) in Fig. 8. The Sn-content in this layer is negligible and the average composition (Pb-20 at.% Pd) falls in the metastable region of the miscibility gap shown in Fig. 11.

vided all phases are solid. The major feature to be noted in Fig. 10 is virtually negligible solid solubility of Pd in (Pb) and (Sn), and the presence of a (Pb)+ $\text{PdSn}_4 + (\text{Sn})$  three-phase field. The microstructure shown in Fig. 3 suggests that the diffusion path in the solid-state follows along (Pb)+(Sn)/ (Pb)+ $\text{PdSn}_4 + (\text{Sn})$ /  $\text{PdSn}_4 + (\text{Pb})$ / $\text{PdSn}_4 + \text{PdSn}_3 + (\text{Pb})$  in Fig. 10. The experimental evidence for the  $\text{PdSn}_4 + (\text{Pb})$  phase field is demonstrated in Fig. 3 where  $\text{PdSn}_4$  in contact with (Pb) (or the region A) may be seen.

We find that the interfacial microstructures for Pb/Pd and 95Pb5Sn/Pd diffusion couples presented in the previous section cannot be understood using calculated equilibrium phase diagrams. For example, in the case liquid-state reaction of the 95Pb5Sn/Pd diffusion couple,  $\text{PdSn}_2$  is predicted to be present at the interface. Even though this phase was observed occasionally,  $\text{PdPb}_2$  phase was observed after both liquid-state and solid-state reaction. In the absence of metastability, the observation of  $\text{PdPb}_2$  at the interface seems to violate the rules of ternary diffusion discussed above.

With respect to the liquid-state reaction of the Pb/Pd diffusion couple, we interpret the lamellar microstructure in Fig. 6 as a result of a metastable eutectic solidification. Figure 11 is a calculated metastable Pb-Pd phase diagram showing the presence of a eutectic reaction in the Pb-rich side. The calculated chemical spinodal boundary is also shown in Fig. 11. The calculated metastable eutectic composition matches very well with the measured Pb/Pd composition close to the interface shown in Fig. 7. We also find almost identical macroscopic alloy composition near the Pd-interface after liquid-state reaction at 343°C for 15 and 35 s. Despite the lack of structural verification at this time, the metastable solidification is further supported by the good agreement between the measured compositions of the eutectic phases and the calculated metastable phase boundaries.

As mentioned earlier, the solid-state reaction of the

95Pb5Sn/Pd diffusion couple develops a continuous layer near the Pd-interface (marked X in Fig. 8a). The macroscopic composition profile across this region is shown in Fig. 12. It may be noted that both Pd- and Sn-contents have decreased compared to their initial values immediately after liquid-state reaction (see Fig. 5). While the Pd-content has decreased from about 30 to 20 at.%, the Sn-content is reduced from about 14 at.% to almost zero. Therefore, the microstructure in this "layer-like growth" region can be understood in terms of the binary Pb-Pd phase diagram. It is to be noted in Fig. 11 that at 125°C, a Pb-20 at.% Pd alloy lies in the metastable region of the miscibility gap. This is consistent with the phase separated microstructure shown in Fig. 8b. Further analysis on the origin of metastable interfacial microstructures involving high-lead solder and palladium and their characterization are in progress.<sup>8</sup>

Finally, the unique self-assembled microstructures shown in Figs. 1 and 2, a direct consequence of the diffusion path, represent a dispersion of a ductile phase (Pb) in a brittle matrix (presumably PdSn<sub>4</sub> and PdSn<sub>3</sub> intermetallics are brittle). This is desirable from a fracture mechanics point of view as it may promote crack blunting and/or crack deflection when a crack passes through this layer. In solder interconnects, it is desirable that the failure lie in the solder and not at the solder-substrate interface. The interfacial microstructure should be designed to prevent failure from occurring at the solder-intermetallic interface.

### CONCLUSIONS

A systematic study of interfacial reaction, both in the liquid- and solid-state, in (62Sn38Pb solder)/Pd,

(9SPbSSn solder)/Pd, and Pb/Pd diffusion couples is reported. The interfacial microstructures are characterized by imaging and quantitative EDS analysis in SEM.

The interfacial microstructures in ternary diffusion couples, with eutectic Pb-Sn solders on Pd, were found to be consistent with the calculated phase diagrams.

In the case of high-lead solder on Pd, a decomposed microstructure was observed. This is due to a metastable eutectic reaction and a metastable miscibility gap in the Pb-Pd system which are carried over to the ternary system. The interfacial microstructures in all diffusion couples are found to be governed by the diffusion of Pd.

### ACKNOWLEDGMENTS

This work was supported by the Semiconductor Research Corporation (Grant # 447G, Grant Monitor: Dr. Ron Bracken) and the National Science Foundation (Grant # DMR-9523447).

### REFERENCES

1. D.C. Abbott, R.M. Brook, N. McLelland and J.S. Wiley, *IEEE Trans. CHMT* 14, 567 (1991).
2. G. Ghosh, to appear in *Metall. Mater. Trans.* (1998).
3. J.S. Kirkaldy and L.C. Brown, *Can. Met. Quart.* 2, 89 (1963).
4. L.S. Castleman, *Metall. Trans. A* 12A, 2031 (1981); 14A, 45 (1983).
5. M.A. Dayananda, *Diffusion in Solids: Recent Developments*, ed. M.A. Dayananda and G.E. Murch, (Warrendale, PA: TMS, 1985), p. 195.
6. J.R. Manning, *Metall. Trans.* 1, 499 (1970).
7. C.R. Kao, J. Woodford, S. Kim, M.-X. Zhang and Y.A. Chang, *Mater. Sci. Eng.* A195, 29 (1995).
8. G. Ghosh, unpublished research, Northwestern University, 1998.